

# Neutral Mononuclear, Dinuclear, Tetranuclear $d^7/d^{10}$ Metal Complexes Containing bis-Pyrazole/Pyridine Ligands Supported by 2,6-bis(3-Pyrazolyl)Pyridine: Synthesis, Structure, Spectra, and Catalytic Activity

Lijuan Wan,<sup>†</sup> Caishun Zhang,<sup>†</sup> Yongheng Xing,<sup>\*,†</sup> Zhen Li,<sup>‡</sup> Na Xing,<sup>†</sup> Liying Wan,<sup>§</sup> and Hui Shan<sup>†</sup>

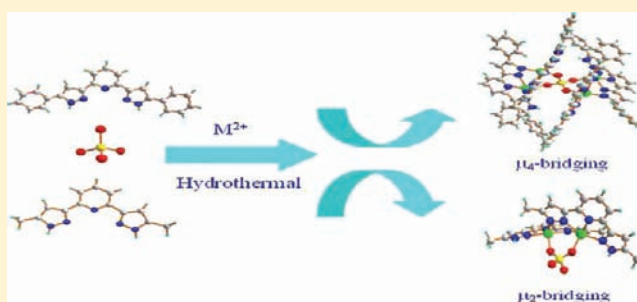
<sup>†</sup>College of Chemistry and Chemical Engineering, Liaoning Normal University, Dalian 116029, P. R. China

<sup>‡</sup>ARC Centre of Excellence for Functional Nanomaterials, Australian Institute for Bioengineering and Nanotechnology, The University of Queensland, Brisbane 4072

<sup>§</sup>School of Software, Dalian University of Foreign Languages, Dalian 116044, P. R. China

## Supporting Information

**ABSTRACT:** A series of novel bis-pyrazole/pyridine complexes,  $[\text{Zn}_2(\text{HL}^1)_2(\mu_2\text{-SO}_4)]_2 \cdot \text{EtOH} \cdot \text{H}_2\text{O}$  (1),  $[\text{Co}_2(\text{HL}^1)_2(\mu_2\text{-SO}_4)]_2 \cdot 2\text{DMF} \cdot 6\text{H}_2\text{O}$  (2),  $[\text{Zn}_4(\text{HL}^1)_4(\mu_4\text{-SO}_4)]_2[\text{OH}]_2$  (3),  $[\text{Zn}_2(\text{HL}^2)_2(\mu_2\text{-SO}_4)] \cdot 2\text{H}_2\text{O}$  (4),  $[\text{Zn}(\text{H}_2\text{L}^2)(\text{H}_2\text{O})_2](\text{SO}_4) \cdot 0.87\text{H}_2\text{O}$  (5) ( $\text{H}_2\text{L}^1 = 2,6\text{-di-(5-phenyl-1H-pyrazol-3-yl)pyridine}$ ,  $\text{H}_2\text{L}^2 = 2,6\text{-di-(5-methyl-1H-pyrazol-3-yl)pyridine}$ ), were synthesized hydrothermally from the self-assembly of Zn(II) or Co(II) with different types of bipyrazolyl/pyridine derivative ligands. All the complexes were characterized by elemental analysis, IR and UV-vis spectroscopy, powder X-ray diffraction (PXRD), and single-crystal X-ray diffraction. Structural analyses revealed that metal atoms (Zn and Co) in complexes 1–5 are five-coordination modes, forming slightly distorted trigonal bipyramidal geometries. In complexes 1–3,  $\text{H}_2\text{L}^1$  ligand connected the two metal centers via the tetradentate fashion, and the same form of connection was found in complex 4 with  $\text{H}_2\text{L}^2$  ligand. While in complex 5,  $\text{H}_2\text{L}^2$  only connected with one metal center via the tridentate fashion, which was different from those in complexes 1–4. Additionally, there are abundant hydrogen bonding interactions in complexes 1–4. Interestingly, for hydrogen bonding connecting fashions being different, the molecules for the complexes 1 and 4 are held together by the hydrogen bond to form a 1D supramolecular structure, whereas complexes 2 and 3 are a hydrogen bonded dimer. In addition, quantum chemical calculations for 1, 3, and 4, thermal behaviors and photoluminescent properties for 1 and 3–5 were performed and discussed in detail. In the mean time, we found that these complexes had potential catalytic activity for the oxidation reaction of cyclohexane.



## INTRODUCTION

The construction of metal–organic networks has emerged as the field of current research interest due to their intriguing variety of topologies and various potential applications as functional materials, i.e. lower density and more convenience in structural modification and incorporation with functionalities like hydrophilicity, hydrophobicity, photoluminescence, and magnetism, etc.<sup>1–4</sup> While the rational design and synthesis of the prospective metal–organic networks with the specific properties can be realized by careful selection of the properties of the ligands, such as shape, functionality, flexibility, symmetry, length, and substituent groups and so on, exploring the rules in the synthesis of porous transition metal complexes remains a difficult mission. Undoubtedly, it is essential to choose suitable bridging ligands and reaction conditions. Among these used ligands, it is worthy to note that the use of rich nitrogen-donor ligands is an effective method to form meaningful metal–organic frameworks, because they can satisfy and even mediate

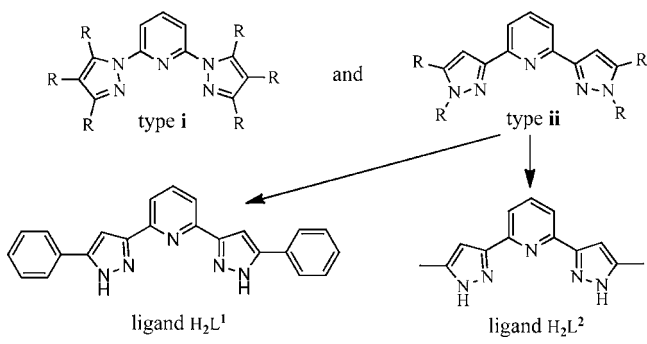
the coordination needs of the metal center.<sup>5,6</sup> The bipyridyl-like compound as the typical heterocyclic ligand with nitrogen donor atom has been extensively employed in the construction of novel architectures. In particular, derivatives of 2,6-di(pyrazol-1-yl)pyridine are widely studied in coordination chemistry.<sup>7–9</sup> This is because (i) the ligand is easy to understand; (ii) it is commercially available or straightforward to synthesize (particularly those substituted at the 3, 4, 5-position on pyrazolyl moiety are also readily accessible); (iii) it can bind to both low- and high-oxidation state metal ions, generally in tridentate fashion.<sup>6,10–12</sup> The properties and the synthetic accessibility of substituted derivatives of 2,6-di(1-pyrazolyl)pyridine have also led to metal-bis(terpy) centers being incorporated into coordination complexes, dendrimers, and other functional supramolecular structures.<sup>13</sup> In general, for

Received: December 26, 2011

Published: June 4, 2012

2,6-di(pyrazolyl) pyridine derivative ligands, there are mainly two types (shown in the Scheme 1) as follows: (i) 2,6-di(1-

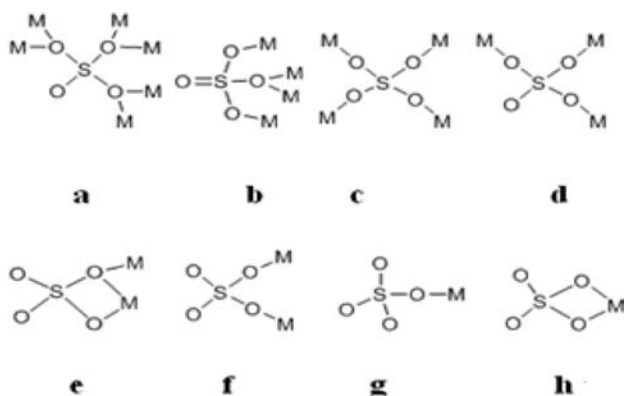
**Scheme 1. Structures of the Type of 2,6-di(Pyrazolyl) Pyridine Derivative Ligands**



pyrazolyl)pyridine derivatives and (ii) 2,6-di(3-pyrazolyl)pyridine derivatives. By comparing type i with ii, type ii can display more coordination modes. This is attributed to five N atoms (one is on the pyridine ring, the other four are on the pyrazolyl rings) to coordinate with metal atoms. When the first position for both the pyrazolyl rings is substituted with H atoms, all of the five N atoms for ligands of the type ii can coordinate with metal atoms and form metal complexes with different structures.<sup>7,8</sup>

To our best knowledge, although much work has been focused on ligands of the type ii to prepare transition metal complexes, only a few kinds of coordination complexes with 2,6-bis(5-phenyl-1H-pyrazol-3-yl)pyridine ( $H_2L^1$ ) or 2,6-bis(5-methyl-1H-pyrazol-3-yl)pyridine ( $H_2L^2$ ) have been synthesized, such as  $H_2L^1$ -Cd,  $H_2L^1$ -Zn,  $L^1$ -Cu,  $H_2L^1$ -Ag,  $H_2L^2$ -Ag,  $L^2$ -Cu, etc. Research results have shown that the complexes containing such ligands above were prepared by different synthetic methods and exhibited different architectures.<sup>7-9</sup> On the other hand, doubly charged anions like sulfates are known to generally participate in coordination of metal complexes. Some remarkable examples of polymeric species containing  $SO_4^{2-}$  anions are reported in recent years, with various coordination modes: (a)  $\mu_6-\eta^2-\eta^2-\eta^2-SO_4$ ,<sup>14</sup> (b)  $\mu_4-\eta^1-\eta^1-\eta^2-SO_4$ ,<sup>15</sup> (c)  $\mu_4-\eta^1-\eta^1-\eta^1-\eta^1-SO_4$ ,<sup>16</sup> (d)  $\mu_3-\eta^1-\eta^1-\eta^1-SO_4$ ,<sup>17</sup> (e)  $\mu_2-\eta^1-\eta^2-SO_4$ ,<sup>18</sup> (f)  $\mu_2-\eta^1-\eta^1-SO_4$ ,<sup>16</sup> (g)  $\mu_1-\eta^1-SO_4$ ,<sup>19</sup> and (h)  $\mu_1-\eta^1-\eta^1-SO_4$ ,<sup>20</sup> as shown in Scheme 2. In particular, types d-g are common coordination modes; however, types a, b, c, and h are rare. Up to now, 2,6-di(3-pyrazolyl)pyridine

**Scheme 2. Coordination Modes of the  $SO_4^{2-}$  Anion**



derivatives ( $H_2L^1/H_2L^2$ ) have rarely been used to prepare metal-organic complexes with interesting structures and functional properties, especially the luminescence of the ligands and the complexes. In addition, we have recently found that some metal complexes with N<sub>2</sub>O- or N<sub>2</sub>N-ligands can catalyze alkane functionalization reactions, under mild or moderate conditions in homogeneous systems using peroxides as an oxidant and exhibit a good catalytic efficiency<sup>21-26</sup> in the partial oxidation of cyclohexane (to cyclohexanol and cyclohexanone), that is a reaction of industrial importance. In order to further extend structural variety and explore catalytic property of transition metal complexes, here, we report synthesis, structure, spectra, and catalysis activity of five new metal-organic complexes, namely  $[Zn_2(HL^1)_2(\mu_2-SO_4)]_2 \cdot EtOH \cdot H_2O$  (1),  $[Co_2(HL^1)_2(\mu_2-SO_4)]_2 \cdot 2DMF \cdot 6H_2O$  (2),  $[Zn_4(HL^1)_4(\mu_4-SO_4)] [OH]_2$  (3),  $[Zn_2(HL^2)_2(\mu_2-SO_4)] \cdot 2H_2O$  (4),  $[Zn(H_2L^2)(H_2O)_2](SO_4) \cdot 0.87H_2O$  (5). Single crystal X-ray diffractions reveal that in the complexes, the  $SO_4^{2-}$  anion shows the two kinds of coordination modes ( $\mu_4-\eta^1-\eta^1-\eta^1-\eta^1$  and  $\mu_2-\eta^1-\eta^1$ ). In addition, the influence of diversified coordination modes of the  $SO_4^{2-}$  anion on photoluminescent properties for the complexes 1 and 3-5 has also been investigated in detail.

## EXPERIMENTAL SECTION

**General Considerations.**  $H_2L^1$  and  $H_2L^2$  were synthesized according to the modified literature method.<sup>8,27,28</sup> A 30% aqueous solution of hydrogen peroxide was used as primary oxidant. All other chemicals purchased were of reagent grade or better and used without further purification. IR spectra was recorded on a JASCO FT/IR-480 PLUS Fourier Transform spectrometer with pressed KBr pellets in the range 200–4000  $cm^{-1}$ . The elemental analyses for C, H, and N were carried out on a Perkin-Elmer 240C automatic analyzer. Thermogravimetric analyses (TGA) were performed under atmosphere with a heating rate of 10  $^{\circ}C/min$  on a Perkin-Elmer Diamond TG/DTA. The luminescence spectra was reported on a JASCO F-6500 spectrofluorimeter (solid). UV-vis absorption spectra diffuse reflection was recorded with a JASCO V-570-UV/vis/NIR spectrophotometer in the 200–2500 nm. X-ray powder diffraction (PXRD) patterns were obtained on a Bruker Advance-D8 equipped with Cu  $K\alpha$  radiation, in the range  $5^{\circ} < 2\theta < 50^{\circ}$ , with a step size of  $0.02^{\circ}$  ( $2\theta$ ) and a count time of 2s per step. The reaction products of oxidation were determined and analyzed by Shimadzu GC-16A series gas chromatograph equipped with a flame ionization detector (FID) and a capillary column with the temperature of injection being 250  $^{\circ}C$ . Nitrogen was used as the carrier gas. In GC calculations, all peaks amounting to at least 0.5% of the total products were taken into account.

**Synthesis.**  $[Zn_2(HL^1)_2(\mu_2-SO_4)]_2 \cdot EtOH \cdot H_2O$  (1).  $ZnSO_4 \cdot 7H_2O$  (28.7 mg, 0.1 mmol),  $H_2L^1$  (36.3 mg, 0.1 mmol), and glutaric acid (200 mg, 1.5 mmol) in water (10 mL), DMF (3 mL), and EtOH (2 mL) were mixed in a 25 mL beaker and stirred for 5 h; the final reaction mixture was sealed in a 25 mL Teflon-lined stainless steel vessel under autogenous pressure and heated at 160  $^{\circ}C$  for 3 days, then followed by slow cooling to room temperature. After filtration, the product was washed with distilled water and then dried at room temperature. Colorless block crystals suitable for X-ray diffraction analysis were obtained. Yield: 46%. Anal. calc. for  $C_{94}H_{72}N_{20}O_{10}S_2Zn_4$  (1967.32): C, 57.34; H, 3.66; N, 14.23. Found: C, 57.31; H, 3.54; N, 14.15%. IR data ( $KBr, cm^{-1}$ ): 3421, 3124, 3064, 2968, 2927, 1612, 1574, 1455, 1396, 1291, 1174, 1112, 1057, 1020, 970, 819, 784, 761, 697, 617, 538, 424. In addition, in order to further investigate function of the glutaric acid in the reaction system, when increasing amounts of glutaric acid to 400 mg (3 mmol), it is found that a new species of Zn-L<sup>1</sup>-glutaric acid complex was formed by checking its IR spectra. However, only producing some microcrystalline products are unsuitable for single crystal X-ray diffraction analysis.

$[Co_2(HL^1)_2(\mu_2-SO_4)]_2 \cdot 2DMF \cdot 6H_2O$  (2).  $CoCl_2 \cdot 6H_2O$  (24.5 mg, 0.103 mmol),  $H_2L^1$  (44.9 mg, 0.124 mmol), water (10 mL), and DMF (5

Table 1. Crystallographic Data for Complexes 1–5

complexes	1	2	3	4	5
formula	C <sub>94</sub> H <sub>72</sub> N <sub>20</sub> O <sub>10</sub> S <sub>2</sub> Zn <sub>4</sub>	C <sub>98</sub> H <sub>90</sub> N <sub>22</sub> O <sub>16</sub> S <sub>2</sub> Co <sub>4</sub>	C <sub>92</sub> H <sub>66</sub> N <sub>20</sub> O <sub>6</sub> SZn <sub>4</sub>	C <sub>26</sub> H <sub>28</sub> N <sub>10</sub> O <sub>6</sub> SZn <sub>2</sub>	C <sub>13</sub> H <sub>18.74</sub> N <sub>5</sub> O <sub>6.87</sub> SZn
<i>M</i> (g mol <sup>-1</sup> )	1967.32	2131.76	1841.19	739.38	452.42
crystal system	triclinic	triclinic	triclinic	monoclinic	monoclinic
space group	$\bar{P}1$	$\bar{P}1$	$\bar{P}1$	<i>C</i> 2/ <i>c</i>	<i>P</i> 2 <sub>1</sub> / <i>n</i>
<i>a</i> (Å)	12.6979(7)	16.6277(11)	14.802(3)	18.430(2)	13.180(3)
<i>b</i> (Å)	17.3289(11)	17.5615(12)	15.162(3)	14.554(2)	6.9337(14)
<i>c</i> (Å)	21.7880(11)	20.0031(13)	18.087(4)	11.2900(17)	19.744(4)
$\alpha$ (deg)	101.311(4)	74.7940(10)	85.68(3)	90	90
$\beta$ (deg)	101.010(4)	66.3760(10)	85.54(3)	103.489(3)	93.74(3)
$\gamma$ (deg)	109.716(3)	66.9580(10)	83.82(3)	90	90
<i>V</i> (Å <sup>3</sup> )	4250.3(4)	4917.1(6)	409.34(11)	2944.8(8)	1800.5(6)
<i>Z</i>	2	2	2	4	4
<i>D</i> <sub>calc</sub> (g cm <sup>-3</sup> )	1.537	1.440	1.523	1.668	1.669
crystal size (mm)	0.317 × 0.098 × 0.066	0.469 × 0.241 × 0.069	0.302 × 0.072 × 0.058	0.612 × 0.201 × 0.278	0.441 × 0.148 × 0.059
<i>F</i> (000)	2016	2200	1884	1512	931
$\mu$ (Mo–K $\alpha$ )/mm <sup>-1</sup>	1.240	0.783	1.278	1.760	1.527
$\theta$ (deg)	1.30–25.00	1.12–25.00	3.01–25.00	2.27–25.00	3.10–27.47
reflections collected	24308	28524	30894	7231	16321
independent reflections	14960	17304	13631	2579	4034
parameters	1170	1279	1108	217	280
$\Delta(\rho)$ (e Å <sup>-3</sup> )	0.790, -0.586	0.842, -0.463	0.504, -0.717	1.051, -0.445	1.12, -0.691
goodness of fit	0.776	0.967	0.972	1.105	1.070
<i>R</i> <sup>a</sup>	0.0594(0.1655) <sup>b</sup>	0.0861(0.1874) <sup>b</sup>	0.0950(0.2164) <sup>b</sup>	0.0353(0.0440) <sup>b</sup>	0.0680(0.0984) <sup>b</sup>
<i>wR</i> <sub>2</sub> <sup>a</sup>	0.1264(0.1497) <sup>b</sup>	0.2431(0.2893) <sup>b</sup>	0.1923(0.2369) <sup>b</sup>	0.0938(0.0979) <sup>b</sup>	0.1806(0.2046) <sup>b</sup>

<sup>a</sup>*R* =  $\sum ||F_o| - |F_c|| / \sum |F_o|$ , *wR*<sub>2</sub> =  $[\sum (w(F_o^2 - F_c^2))^2 / \sum (w(F_o^2))^2]^{1/2}$ ; [*F*<sub>o</sub> > 4 $\sigma$ (*F*<sub>o</sub>)]. <sup>b</sup>Based on all data.

Table 2. Selected Bond Distances (Å) of Complexes 1–5

Complex 1							
Zn1–O1	1.978(5)	Zn2–O2	1.988(5)	Zn3–O5	1.987(5)	Zn4–O6	1.976(5)
Zn1–N1	2.024(5)	Zn2–N6	2.002(5)	Zn3–N20	2.033(5)	Zn4–N15	1.997(6)
Zn1–N8	2.128(5)	Zn2–N3	2.107(5)	Zn3–N13	2.115(5)	Zn4–N18	2.091(5)
Zn1–N7	2.149(6)	Zn2–N2	2.124(6)	Zn3–N14	2.148(6)	Zn4–N19	2.187(5)
Zn1–N9	2.304(7)	Zn2–N4	2.153(6)	Zn3–N12	2.252(6)	Zn4–N17	2.192(6)
Complex 2							
Co1–O1	1.972(8)	Co2–O2	1.991(9)	Co3–O6	1.959(9)	Co4–O5	1.988(9)
Co1–N1	2.005(10)	Co2–N6	2.021(9)	Co3–N11	2.007(10)	Co4–N16	2.027(10)
Co1–N8	2.050(9)	Co2–N3	2.054(9)	Co3–N18	2.070(10)	Co4–N13	2.076(9)
Co1–N7	2.080(9)	Co2–N2	2.116(10)	Co3–N17	2.123(11)	Co4–N12	2.120(9)
Co1–N9	2.109(10)	Co2–N4	2.106(10)	Co3–N19	2.150(11)	Co4–N14	2.142(9)
Complex 3							
Zn1–N1	2.051(7)	Zn2–N6	1.983(8)	Zn3–N16	2.021(7)	Zn4–N11	1.973(8)
Zn1–O1	2.055(6)	Zn2–O2	2.030(6)	Zn3–O3	2.041(6)	Zn4–O4	2.030(6)
Zn1–N9	2.089(9)	Zn2–N3	2.067(7)	Zn3–N13	2.085(8)	Zn4–N18	2.078(7)
Zn1–N8	2.091(9)	Zn2–N4	2.165(8)	Zn3–N4	2.088(8)	Zn4–N17	2.145(8)
Zn1–N7	2.162(9)	Zn2–N2	2.188(7)	Zn3–N12	2.215(8)	Zn4–N19	2.185(8)
Complex 4							
Zn1–O1	1.988(2)	Zn1–N5	2.000(3)	Zn1–N3	2.117(3)	Zn1–N4	2.130(3)
Zn1–N2	2.193(3)						
Complex 5							
Zn–O1	1.967(4)	Zn–O2	1.973(4)	Zn–N3	2.073(4)	Zn–N4	2.175(4)
Zn–N2	2.178(5)						

mL) were mixed in a 25 mL beaker and stirred for 4 h with the pH value 5–6 adjusted by the solution of 2 M H<sub>2</sub>SO<sub>4</sub>. The final reaction mixture was sealed in a 25 mL Teflon-lined stainless steel vessel under autogenous pressure and heated at 180 °C for 3 days, then followed by slow cooling to room temperature. After filtration, the product was washed with distilled water and then dried at room temperature. Dark red block crystals suitable for X-ray diffraction analysis were obtained

. Yield: 16%. Anal. calc. for C<sub>98</sub>H<sub>90</sub>N<sub>22</sub>O<sub>16</sub>S<sub>2</sub>Co<sub>4</sub> (2131.76): C, 55.17; H, 4.22; N, 14.45. Found C, 54.78; H, 3.98; N, 13.85%. IR data (KBr, cm<sup>-1</sup>): 3422, 3121, 3062, 2923, 2852, 1669, 1640, 1612, 1570, 1454, 1386, 1289, 1159, 1113, 1079, 1018, 970, 815, 782, 760, 695, 617, 538, 426.

[Zn<sub>4</sub>(HL<sup>1</sup>)<sub>4</sub>(μ<sub>4</sub>-SO<sub>4</sub>)] [OH]<sub>2</sub> (**3**). Complex **3** was obtained by hydrothermal procedure as that for preparation of **2** just using ZnSO<sub>4</sub>·7H<sub>2</sub>O

(28.7 mg, 0.1 mmol) instead of  $\text{CoCl}_2 \cdot 6\text{H}_2\text{O}$  as the starting reactant and heating at 160 °C for 3 days. Colorless block crystals of **3** were collected. Yield: 65%. Anal. calc. for  $\text{C}_{92}\text{H}_{66}\text{N}_{20}\text{O}_6\text{SZn}_4$  (1841.19): C, 60.00; H, 3.58; N, 15.21. Found: C, 59.68; H, 3.49; N, 15.15%. IR data (KBr,  $\text{cm}^{-1}$ ): 3492, 3061, 1612, 1574, 1456, 1289, 1152, 1107, 1022, 970, 808, 783, 759, 695, 597, 529, 425.

$[\text{Zn}_2(\text{HL}^2)(\mu_2\text{-SO}_4)] \cdot 2\text{H}_2\text{O}$  (**4**).  $\text{ZnSO}_4 \cdot 7\text{H}_2\text{O}$  (28.7 mg, 0.1 mmol) and  $\text{H}_2\text{L}^2$  (23.9 mg, 0.1 mmol) in water (10 mL) and EtOH (5 mL) were mixed in a 25 mL beaker and stirred. After 5 h, the final reaction mixture was sealed in a 25 mL Teflon-lined stainless steel vessel under autogenous pressure and heated at 145 °C for 3 days, then followed by slow cooling to room temperature. After filtration, the product was washed with distilled water and then dried at room temperature. Yellow block crystals suitable for X-ray diffraction analysis were obtained. Yield: 56%. Anal. calc. for  $\text{C}_{26}\text{H}_{28}\text{N}_{10}\text{O}_6\text{SZn}_2$  (739.38): C, 42.20; H, 3.79; N, 18.93. Found: C, 42.16; H, 3.70; N, 18.84%. IR data (KBr,  $\text{cm}^{-1}$ ): 3419, 3124, 3080, 2927, 2856, 1612, 1577, 1490, 1448, 1337, 1288, 1155, 1116, 1069, 1015, 820, 797, 781, 659, 619, 489, 352.

$[\text{Zn}(\text{H}_2\text{L}^2)(\text{H}_2\text{O})_2] \cdot (\text{SO}_4) \cdot 0.87\text{H}_2\text{O}$  (**5**).  $\text{ZnSO}_4 \cdot 7\text{H}_2\text{O}$  (28.7 mg, 0.1 mmol),  $\text{H}_2\text{L}^2$  (23.9 mg, 0.1 mmol), and adipic acid (102.2 mg, 0.7 mmol) in water (10 mL) and EtOH (5 mL) were mixed in a 25 mL beaker and stirred. After 4 h, the final reaction mixture was sealed in a 25 mL Teflon-lined stainless steel vessel under autogenous pressure and heated at 145 °C for 3 days, followed by slow cooling to room temperature. Clear solution was given, and then stood for several days. Some yellow crystals were obtained from mother solution. Yield: 45%. Anal. calc. for  $\text{C}_{13}\text{H}_{18.74}\text{N}_5\text{O}_{6.87}\text{SZn}$  (452.42): C, 34.48; H, 4.14; N, 15.47. Found: C, 34.29; H, 4.06; N, 15.32%. IR data (KBr,  $\text{cm}^{-1}$ ): 3440, 3227, 3127, 3073, 2929, 2857, 1615, 1578, 1510, 1437, 1282, 1237, 1120, 1008, 978, 823, 806, 732, 618, 357.

**X-ray Crystallographic Determination.** Suitable single crystals of the five complexes were mounted on glass fibers for X-ray measurement, respectively. Reflection data were collected at room temperature on a Rigaku R-AXIS RAPID IP diffractometer with graphite monochromatized Mo  $K\alpha$  radiation ( $\lambda = 0.71073$  Å). All absorption corrections were performed using the SADABS program.<sup>29</sup> Crystal structures were solved by the direct method. All non-hydrogen atoms were refined anisotropically. All Hydrogen atoms of  $\text{H}_2\text{L}$ , EtOH, and DMF were fixed at calculated positions with isotropic thermal parameters, while hydrogen atoms of the coordinated water molecules, lattice water molecules, and hydroxyl ion were located by difference Fourier map. In particular, for complex **5**,  $\text{SO}_4^{2-}$  is found to be disordered and modeled over two split positions with occupancies in ratio of 0.87:0.13, for O101 and O201, O102 and O202, O103 and O203, respectively. All calculations were performed using the SHELX-97 program.<sup>30</sup> Crystal data and details of the data collection and the structure refinement of complexes **1–5** are given in Table 1. The selected bond lengths of complexes **1–5** are listed in Table 2. Bond distances and angles of hydrogen bonds in complexes **1–4** are presented in Table 3. The drawings were made with Diamond 3.2.

**Methods of Quantum Chemistry Calculation.** B3LYP (Becke three-parameter hybrid functional combined with Lee–Yang–Parr correlation functional)<sup>31,32</sup> calculations were carried out for the complexes **1**, **3**, and **4** with the Gaussian 03 program.<sup>33</sup> The calculation included 95, 185, and 67 atoms; 958, 1842, and 662 basis functions; and 1938, 3712, and 1346 primitive Gaussians for complexes **1**, **3**, and **4**, respectively. The parameters of the molecular structures come from the crystal structure data, and the molecular point groups and their symmetry (Cs) are also considered. The Hay–Wadt LANL2DZ ECP basis set<sup>34</sup> was used for transition metal zinc, and standard 6-31G(d), for the other atoms. Natural bond orbital (NBO) analysis was performed to determine the constitutions and the energies of the molecular orbitals (Supporting Information Table S1) as well as the electronic structures and the bonding characters (Supporting Information Table S2).

**Experimental Setup for Catalytic Oxidation.** The oxidation reactions were carried out under air condition (atmospheric pressure) in Schlenk tubes. In a typical experiment, 0.0004 g of the catalyst (complexes **1–5**) was dissolved in 3.00 mL of desired solvent. Then, the required amounts of  $\text{H}_2\text{O}_2$  (30%  $\text{H}_2\text{O}_2$  solution) and  $\text{HNO}_3$  were

**Table 3.** Bond Distances (Å) and Angles (deg) of Hydrogen Bonds in Complexes **1–4**

D–H...A	$d(\text{D–H})$ Å	$d(\text{H...A})$ Å	$d(\text{D...H})$ Å	$\angle\text{DHA}$ (deg)
complex 1				
O9–H9...O4	0.8200	1.9962	2.7492	152.37
N5–H5A...O9	0.8600	1.9513	2.7398	151.86
N10–H10A...O8	0.8600	1.8785	2.7295	170.02
N11–H11A...O3	0.8600	1.9463	2.7964	169.55
N16–H16A...O1W	0.8600	2.0630	2.8411	150.09
C35–H35...O7	0.9300	2.4273	3.2507	147.56
complex 2				
O2W–H2WA...O10	0.8999	1.9811	2.7670	145.03
O3W–H3WB...O7	0.9001	1.9372	2.8067	161.92
O6W–H6WA...O8	0.8999	2.2646	2.9300	130.49
N5–H5B...O2W	0.8600	1.9843	2.7720	151.77
N15–H15A...O1W	0.8600	1.9771	2.7578	150.40
N20–H20A...O6W	0.8600	2.0842	2.8685	151.31
N10–H10A...O9	0.8600	1.9106	2.7511	165.28
C46–H46A...O4	0.9300	2.4159	3.3241	165.38
C62–H62A...O8	0.9300	2.4625	3.3635	163.19
C69–H69A...O8	0.9300	2.4549	3.3768	171.09
C42–H42A...O9	0.9300	2.5741	3.4132	150.31
complex 3				
O1W–H1WA...O1	0.8199	2.2279	2.9240	142.90
N5–H5A...O2W	0.8600	1.9683	2.7537	151.28
N10–H10A...O1W	0.8600	2.0694	2.8012	142.53
N15–H15A...O2W	0.8600	2.1531	2.7646	127.76
N20–H20A...O1W	0.8600	1.9135	2.7219	156.05
C82–H82A...O4	0.9300	2.5790	3.3762	144.05
complex 4				
O1W–H1WA...O2	0.8466	2.3497	3.1563	159.41
N1–H1D...O1W	0.7154	2.0765	2.7565	159.04
O1W–H1WB...O2	0.8329	1.9789	2.8033	170.24
C1–H1A...O1W	0.9600	2.5749	3.2992	132.39

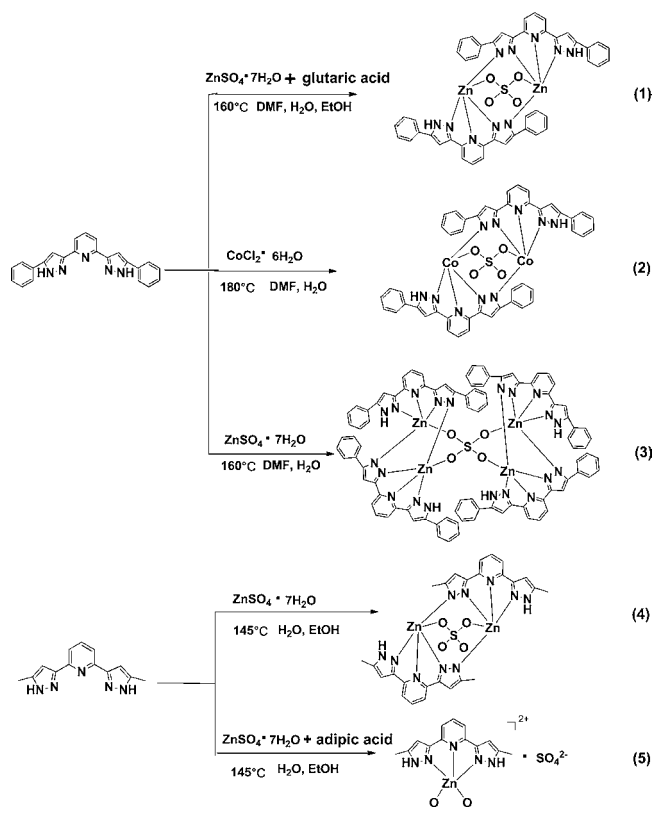
added according to this order. At last, 0.34 g of cyclohexane was added into the solution to make the cyclohexane/catalyst molar ratio equal 15 000. The reaction solution was stirred for some time at the given temperature.

For the product analysis, 0.05 g of methylbenzene (internal standard) and 3 mL of diethyl ether (to extract the substrate and the organic products from the reaction mixture) were added. The obtained mixture was stirred for 10 min, and then, a sample (0.8  $\mu\text{L}$ ) was taken from the organic phase and analyzed by a GC equipped with a capillary column and a flame ionization detector by the internal standard method. Blank experiments confirmed that no cyclohexanol or cyclohexanone are formed in the absence of the metal catalyst under the same conditions.

## RESULTS AND DISCUSSION

**Synthesis.** By the hydrothermal reaction method, complexes **1–5** have been successfully prepared for the first time (Scheme 3). To meet the coordinated condition of  $\text{H}_2\text{L}^1$  or  $\text{H}_2\text{L}^2$  ligand and  $\text{SO}_4^{2-}$  anion with metal atom together in the reaction system, herein we have done our endeavor to search for the optimistic reaction conditions. We initially used diluted sulfate acid solution (2M) to adjust the pH value from 4 to 5 via the reaction of metal salt ( $\text{CoCl}_2 \cdot 6\text{H}_2\text{O}$  or  $\text{ZnSO}_4 \cdot 7\text{H}_2\text{O}$ ) and  $\text{H}_2\text{L}^1$  ligand with molar ratio 1:1 in the mixed system of water and DMF at 180 or 160 °C for 3 days, respectively. Under this condition, we could not obtain the single crystals of the corresponding complexes. Then we readjusted solution pH value to 5–6 and successfully got single crystals of complexes **2**

Scheme 3. Reaction Process of Complexes 1–5



and 3. The results show that the pH value is an important reaction parameter of the crystal growing in the reaction system. To extend diversity of M–L–SO<sub>4</sub> complexes and compare their structural characterization, we attempted to change H<sub>2</sub>L<sup>1</sup> into H<sub>2</sub>L<sup>2</sup> ligand (the structures of H<sub>2</sub>L<sup>1</sup> and H<sub>2</sub>L<sup>2</sup> ligand are very similar and the only difference is the substituent group on the pyrazolyl ring). When the mol ratio of starting material (ZnSO<sub>4</sub>·7H<sub>2</sub>O) and H<sub>2</sub>L<sup>2</sup> ligand is still 1:1 and the pH value of the solution is 5 to 6, the desired product of an M–L–SO<sub>4</sub> system was yet not observed in the mixed system of water and DMF at 145 °C for 3 days. Later, by changing the solvent into the mixture of EtOH and water, we obtained objective complex 4 under the same condition. Through the result of these experiments, we found that not only the pH value of the solution is a very sensitive reaction parameter, but the reaction medium also seems to be one of the vital factors for preparation of the M–L–SO<sub>4</sub> complexes.

In the synthetic process of M–L–SO<sub>4</sub> system complexes, it is found that introduction of aliphatic dicarboxylic acid could affect the coordination of sulfate anion. With increasing the

amount of flexible aliphatic dicarboxylic acid ligand (e.g., adipate or glutaric acid, etc.), it is not in favor of coordination of SO<sub>4</sub><sup>2-</sup> with metal atom, namely, numbers of oxygen atoms from sulfate anion participating in coordination to metal atoms decreased, implying that aliphatic dicarboxylic acid could induce a directing function in the reaction course.

Additionally, powder X-ray diffraction (PXRD) for the complexes 1 and 3–5 was used to confirm the phase purity of the bulk samples. As shown in Supporting Information Figure S1–S4, all the peaks presented in the measured patterns closely match in the simulated patterns generated from single crystal diffraction data.

**IR Spectra.** For complex 1, a broad absorption band appearing at 3421 cm<sup>-1</sup> indicates the presence of water molecules. Absorption at 3124 cm<sup>-1</sup> should be assigned to the stretching vibrations of the N–H on the pyrazolyl rings. The peak appears at 3064 cm<sup>-1</sup> because of the C–H stretching vibrations of the pyridine/pyrazolyl rings. The bands at 2968 and 2927 cm<sup>-1</sup> are characteristic peaks of the C–H (–CH<sub>3</sub>). The bands at 1612, 1574, 1455, 1291, and 1020 cm<sup>-1</sup> are attributed to the characterization stretching vibration of the pyrazolyl and pyridine rings. The characteristic bands of stretching vibrations and bending vibrations of SO<sub>4</sub><sup>2-</sup> anion are in the range of 1020–1112 and 617 cm<sup>-1</sup>, respectively, indicating the coordination feature of the SO<sub>4</sub><sup>2-</sup> anion when coordinated to the metal center. In addition, the detailed appointments of the IR spectra data for the complexes 2–5 are shown in Table 4.

**Structural Descriptions of Complexes 1–5.** *Structural Analyses of Complexes 1–3.* Complexes 1–3 are crystallized in the triclinic system with the  $\bar{P}1$  space group. X-ray single crystal analysis indicates that the asymmetric unit of the complex 1 is made up of two Zn<sub>2</sub>((HL<sup>1</sup>)<sub>2</sub>(SO<sub>4</sub>)) molecules, one lattice ethanol molecule, and one lattice water molecule. The two [Zn<sub>2</sub>((HL<sup>1</sup>)<sub>2</sub>(SO<sub>4</sub>))] molecules (Figure 1a) are very similar, and there is only a little difference on their corresponding bond distances and angles. Moreover, the composition of the complex 2 is similar to that of the complex 1. However, the metal atoms and lattice solvent molecules in the composition of the two complexes are different (Figure 2a). The asymmetric unit of the complex 3 consists of four Zn atoms, four HL<sup>1</sup> ligands, one sulfate anion, and two hydroxide ions (Figure 3a). The coordination environments of the central metal atom (Zn/Co) in the complexes 1–3 are similar. Each central metal atom (Zn/Co) is five-coordinated by four N atoms from two HL<sup>1</sup> ligands and one O atom from one SO<sub>4</sub><sup>2-</sup> anion to form a distorted trigonal bipyramidal geometry, which is best described as trigonal bipyramidal by the structural parameter  $\tau = 0.67$  for 1, 0.77 for 2, and 0.70 for 3, respectively;  $\tau = (\beta - \alpha)/60$ , where  $\alpha$  and  $\beta$  are the largest angles ( $\beta > \alpha$ )

Table 4. Detailed Attribution of IR (cm<sup>-1</sup>) for Complexes 1–5

complexes	1	2	3	4	5
$\nu_{(\text{O}-\text{H})}$	3427	3422	3492	3419	3440
$\nu_{(\text{Ar}-\text{H})}$	3064	3062	3061	3080	3073
$\nu_{(\text{N}-\text{H})}$	3124	3121	3133	3124	3227, 3127
$\nu_{\text{as}}(-\text{CH}_3)$	2927, 2856	2923, 2852		2927, 2856	2929, 2857
pyridine/pyrazolyl	1612, 1574, 1455,1291,	1612, 1570, 1454,1289,	1612, 1574, 1456,1289,	1612, 1577, 1448,1288,	1615, 1578, 1437,1282,
$\nu_{\text{S}-\text{O}}$	1112, 1020	1107, 1018	1107, 1022	1116, 1015	1120, 1008
$\delta_{\text{S}-\text{O}}$	617	617	597	619	618

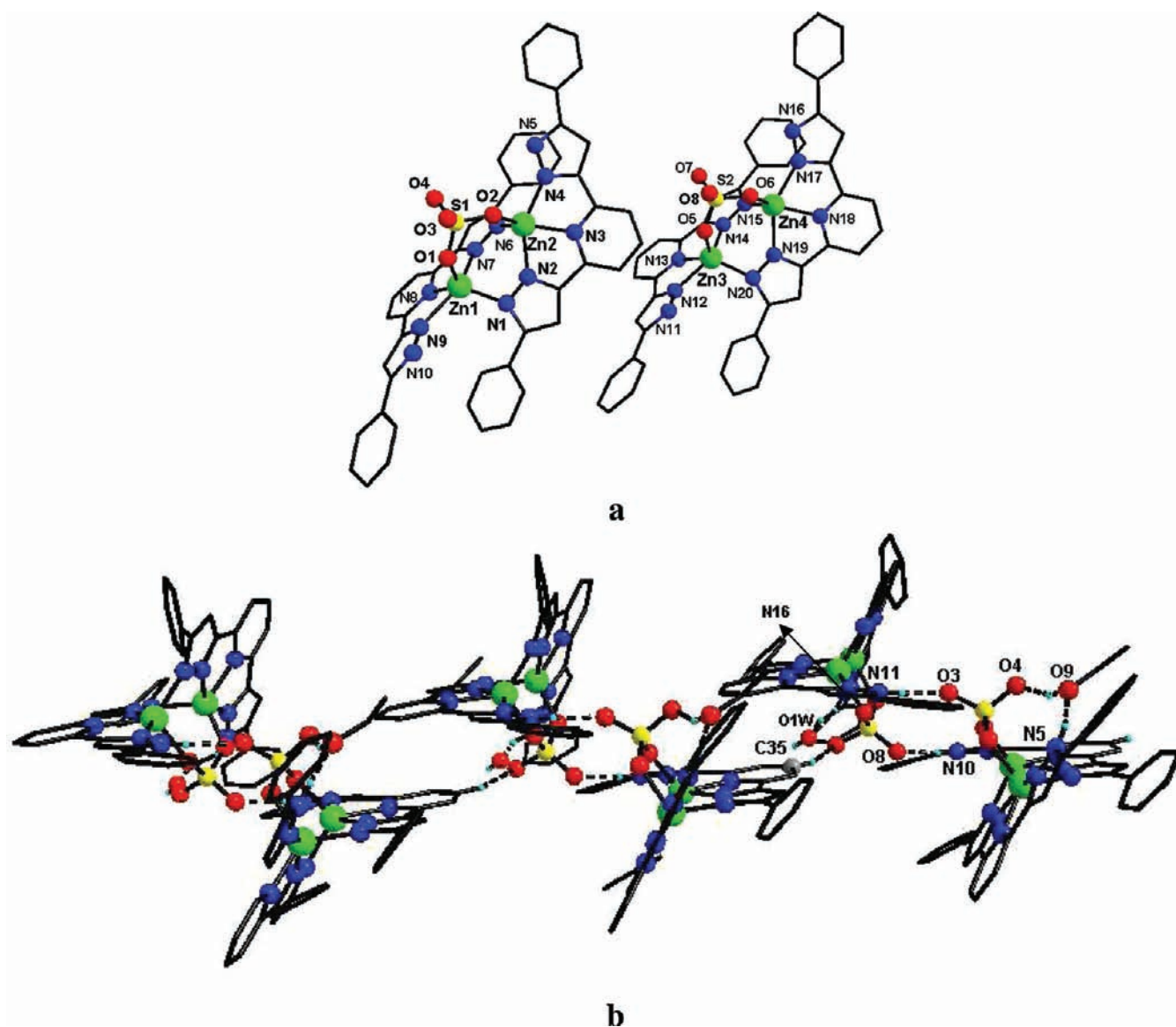


**Figure 1.** (a) Asymmetric unit of the complex **1** (the hydrogen atoms, the lattice ethanol molecule, and the water molecule have been omitted for clarity). (b) View of the hydrogen bonds of the complex **1** (a part of hydrogen atoms are omitted for clarity).

around a five-coordinate metal center, as reported by Addison et al.<sup>35</sup> In the molecular structures, the two closest metal atoms (Zn/Co) are linked by four N atoms from two pyrazolyl rings of the two  $(HL^1)^-$  ligands and two oxygen atoms of a sulfate anion ( $\mu_2-O_2SO_2$ ) to form a mixed three-bridging binuclear structure. The  $(HL^1)^-$  ligand for complexes **1–3** coordinates to two Zn (Co) atoms generating a  $\mu_2-\eta^1-\eta^1-\eta^1-\eta^1$  coordination fashion (Supporting Information Figure S12a). The pyrazolyl rings in the  $(HL^1)^-$  ligand are slightly twisted from the pyridine ring with the dihedral angles ranging from  $1.57(0.44)$  to  $12.12(0.36)^\circ$ . Pyrazolyl rings from two sides are distorted to the least-squares plane (central pyridyl ring) with dihedral angle varying from  $3.69(0.48)$  to  $9.09(0.44)^\circ$ . The sulfate anion of complexes **1** and **2** as a  $\mu_2$ -bridging linker is in the form of  $\mu_2-\eta^1-\eta^1$  mode (Scheme 2f). The uncoordinated S–O bond length is slightly shorter than the coordinated S–O bond length except that the uncoordinated S1–O4 bond length is slightly longer than the coordinated S1–O2 and S2–O6 bond length in complex **2**. While coordinated sulfate group in complex **3** adopts a  $\mu_4$ -bridging coordination mode ( $\mu_4-\eta^1-\eta^1-\eta^1-\eta^1$ ) to link

four Zn atoms (Scheme 2c). In complex **1**, the Zn–N distance ranges from  $1.997(6)$  to  $2.304(7)$  Å and the Zn–O bond length is in the range of  $1.976(5)$ – $1.988(5)$  Å. The angles of the N–Zn–N are in the range of  $73.7(2)$ – $150.1(2)^\circ$ . In complex **3**, the Zn–N distance ranges from  $1.973(8)$  to  $2.215(8)$  Å, and the Zn–O bond length is in range of  $2.030(6)$ – $2.055(6)$  Å; all of which are slightly longer than those corresponding the Zn–N ( $1.985$ – $2.014$  Å) and Zn–O ( $1.898$ – $1.945$  Å) reported in the similar complexes.<sup>36</sup> The angles of the N–Zn–N are in the range of  $74.6(3)$ – $151.6(3)^\circ$ , which is close to those of **1**. In complex **2**, the angles of the N–Co–N are in the range of  $75.5(4)$ – $153.4(4)^\circ$ , which are slightly larger than those of **1** and **3**. The Co–N distances range from  $2.005(10)$  to  $2.150(11)$  Å, and the Co–O bond lengths are in the range of  $1.959(9)$ – $1.988(9)$  Å. These bond lengths are shorter than those observed in the related Co–N and Co–O donor complexes.<sup>37</sup>

In complexes **1–3**, there are three kinds of hydrogen bonds: (i) O–H $\cdots$ O type between the oxygen (donor) from lattice water or ethanol molecule and oxygen (acceptor) from sulfate

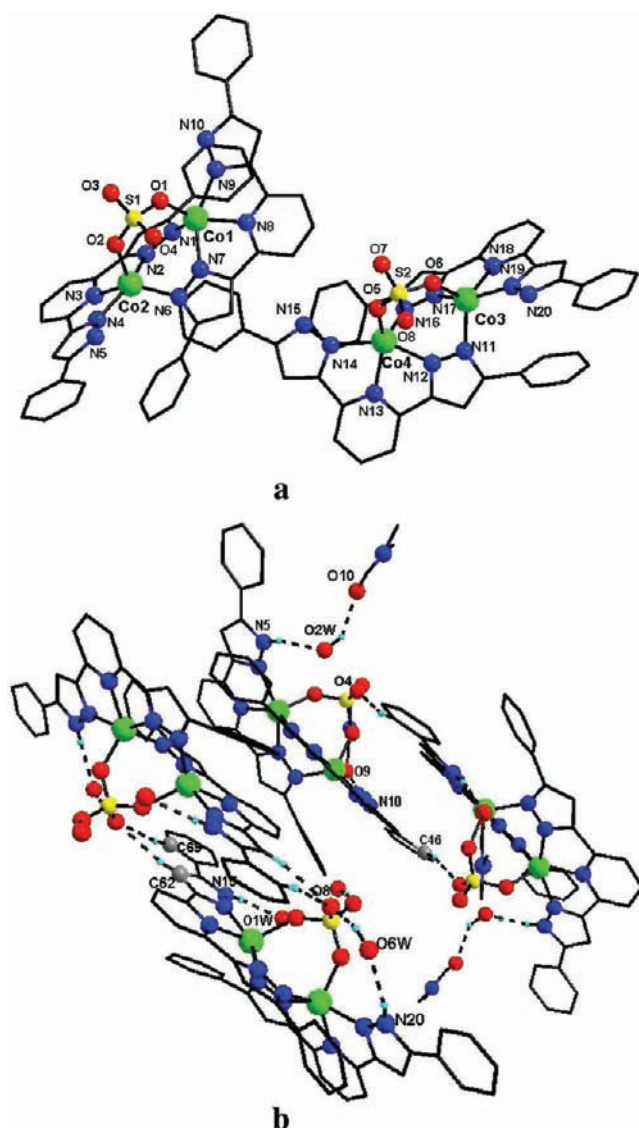


**Figure 2.** (a) Asymmetric unit of the complex 2 (the hydrogen atoms, DMF, and the lattice water molecules have been omitted for clarity). (b) View of the hydrogen-bonded dimer in the complex 2 (a part of hydrogen atoms are omitted for clarity).

group or DMF; (ii) N–H...O type of uncoordinated nitrogen (donor) from (HL<sup>1</sup>)<sup>−</sup> ligand with oxygen atom (acceptor) from lattice water, the ethanol molecule, sulfate group, DMF, or hydroxide group; (iii) C–H...O type of carbon atom (donor) from (HL<sup>1</sup>)<sup>−</sup> ligand with the oxygen atom (acceptor) from sulfate anion, the ethanol molecule or DMF. The molecules in complex 1 are connected by the three types of the hydrogen bonds to form an infinite chain (Figure 1b); however, two adjacent molecules in complex 2 or 3 were connected to form a dimer molecule by the hydrogen bonds above (Figure 2b and 3b). In the mean time, those hydrogen bonds in the complexes 1–3 further enhance the stability of the molecular structures.

**Structural Analysis of [Zn<sub>2</sub>(HL<sup>2</sup>)<sub>2</sub>(SO<sub>4</sub>)]·2H<sub>2</sub>O (4).** X-ray single crystal study shows that complex 4 is crystallized in a monoclinic system with C2/c space group. The asymmetry unit contains one Zn atom, one (HL<sup>2</sup>)<sup>−</sup> ligand, an half sulfate anion, and one lattice water. Zn(II) atom is five-coordinated by four N atoms (N2, N3, N4, N5) from two (HL<sup>2</sup>)<sup>−</sup> ligands and one oxygen atom from one sulfate anion, displaying a distorted

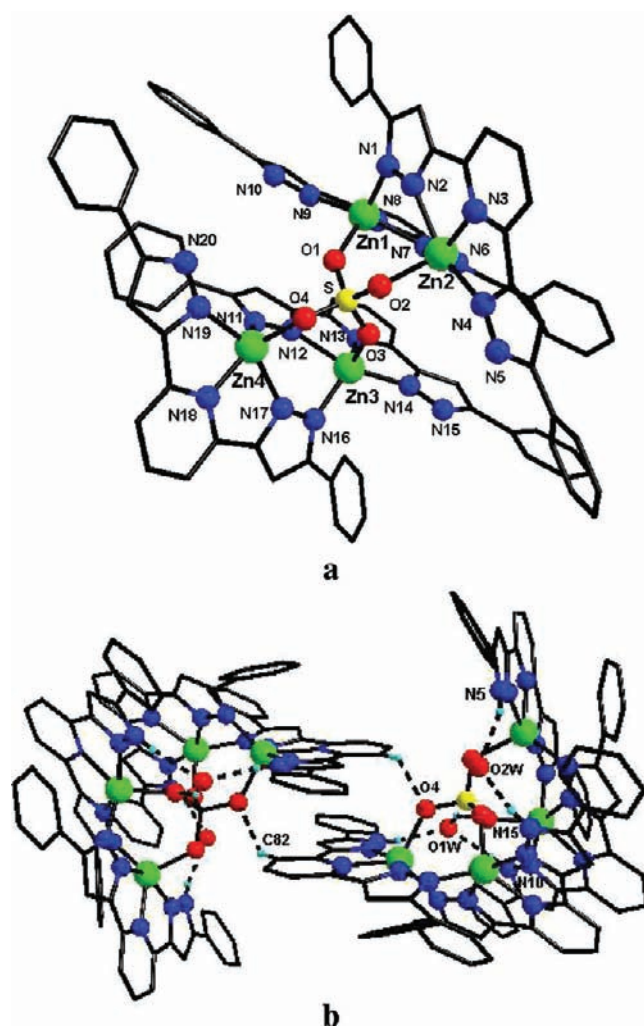


**Figure 3.** (a) Asymmetric unit of the complex 3 (the hydrogen atoms and hydroxide ions have been omitted for clarity). (b) View of the hydrogen-bonded dimer in the complex 3 (a part of hydrogen atoms are omitted for clarity).

trigonal bipyramidal geometry (Figure 4a), which is best described as trigonal bipyramidal by the structural parameter  $\tau = 0.72$  for 4;  $\tau = (\beta - \alpha)/60$ , where  $\alpha$  and  $\beta$  are the largest angles ( $\beta > \alpha$ ) around a five-coordinate metal center, as reported by Addison et al.<sup>35</sup> The HL<sup>2</sup> ligand acts as a  $\mu_2$ -bridging coordination mode to link two Zn atoms in a  $\mu_2$ - $\eta^1$ - $\eta^1$ - $\eta^1$ - $\eta^1$  mode (Supporting Information Figure S12b). The coordination mode of sulfate anion is similar to that of sulfate anion in complexes 1 and 2 ( $\mu_2$ -bridging, Scheme 2f). The coordinated S–O1 bond distance (1.450 Å) is longer than the uncoordinated S–O2 bond distance (1.422 Å). The bond length of Zn–O is 1.988(2) Å, the bond lengths of Zn–N are in the range of 2.000(3)–2.193(3) Å. The angles of the N–Zn–N are in the range of 73.57(10)–148.36(17)°.

Neighborhood molecules are connected by the weak hydrogen bonds involving sulfate anion, lattice water molecule, and the NH group of the pyrazolyl ring from (HL<sup>2</sup>)<sup>−</sup> ligand. Two oxygen atoms from two sulfate anions and two oxygen atoms from two lattice water molecules formed a four-membered ring via weak hydrogen bond interaction of O–H...O and further connected it to generate a 1D chain hydrogen bond network structure (Figure 4b).

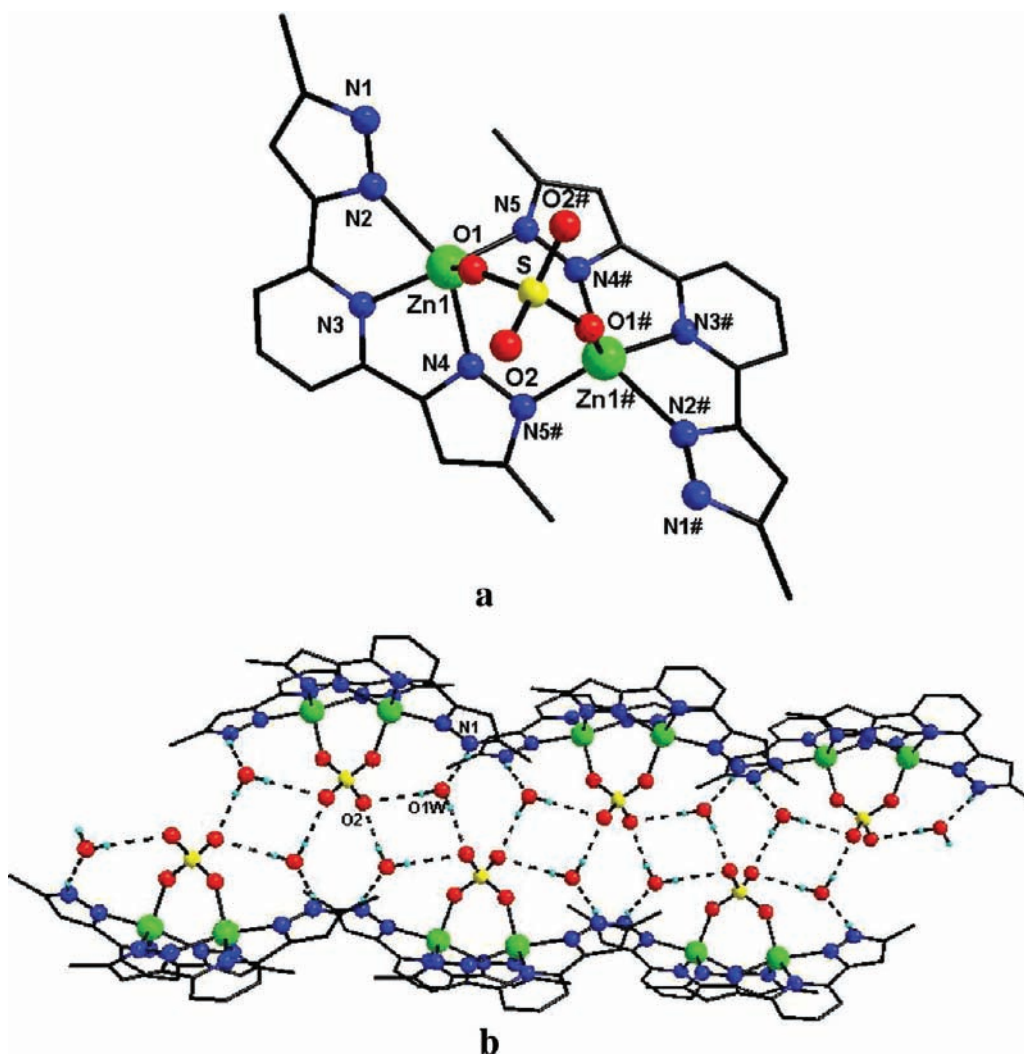


**Figure 4.** (a) Coordination environments of Zn atoms in complex 4 (the hydrogen atoms and the lattice water molecules have been omitted for clarity. Symmetry code no.:  $-x, y, 0.5 - z$ ). (b) View of the hydrogen bonds network of the complex 4 (a part of hydrogen atoms are omitted for clarity).

Structural analyses of  $[\text{Zn}(\text{H}_2\text{L}^2)(\text{H}_2\text{O})_2] \cdot (\text{SO}_4) \cdot 0.87\text{H}_2\text{O}$  (5) X-ray diffraction analysis reveals that complex 5 is crystallized in a monoclinic system with  $P2_1/n$  space group. The asymmetry unit of complex 5 is composed by one Zn atom, one  $\text{H}_2\text{L}^2$  ligand, two coordinated water molecules, one free sulfate anion, and 0.87 lattice water molecule. The coordination environment of the Zn atom is shown in Figure 5. The Zn atom is pentacoordinated in a distorted trigonal bipyramidal geometry around one nitrogen atom from pyridyl, two nitrogen atoms from two pyrazolyls, and two oxygen atoms from two water molecules, which is best described as trigonal bipyramidal by the structural parameter  $\tau = 0.70$  for 5;  $\tau = (\beta - \alpha)/60$ , where  $\alpha$  and  $\beta$  are the largest angles ( $\beta > \alpha$ ) around a five-coordinate metal center, as reported by Addison et al.<sup>35</sup> As expected,  $\text{H}_2\text{L}^2$  acts as a tridentate ligand (Supporting Information Figure S12c). The two axial  $\text{Zn}-\text{N}_{\text{pyrazolyl}}$  bonds (2.175(4) and 2.178(5) Å) are also much longer than that of the equatorial  $\text{Zn}-\text{N}_{\text{pyridyl}}$  bond (2.073(4) Å). The angles of  $\text{N}-\text{Zn}-\text{N}$  are in the range of 75.74(17)–151.48(17)°.

In complex 1, the average bond lengths of  $\text{Zn}-\text{N}_{\text{terminal(pyrazolyl)}}$ ,  $\text{Zn}-\text{N}_{\text{pyridine}}$ , and  $\text{Zn}-\text{N}_{\text{bridge(pyrazolyl)}}$  are 2.225(6), 2.110(5), and 2.083(6) Å, respectively, which show that the order of the bond lengths is  $\text{Zn}-\text{N}_{\text{terminal(pyrazolyl)}} >$

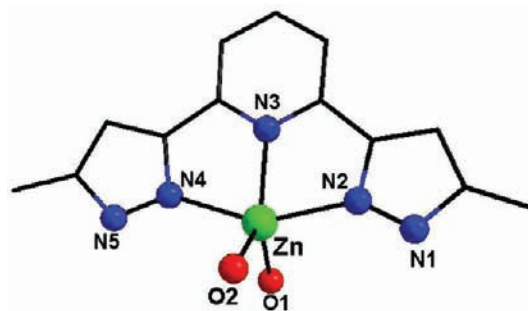


**Figure 5.** Asymmetric unit of the complex 5 (the sulfate group, hydrogen atoms, and the lattice water molecule are omitted for clarity).

$\text{Zn}-\text{N}_{\text{pyridine}} > \text{Zn}-\text{N}_{\text{bridge(pyrazolyl)}}$ . The average bond lengths of  $\text{Zn}-\text{N}$  in complexes 2 and 4 are similar with that of  $\text{Zn}-\text{N}$  in complex 1. However, in complex 3,  $\text{Zn}-\text{N}_{\text{terminal(pyrazolyl)}} > \text{Zn}-\text{N}_{\text{bridge(pyrazolyl)}} > \text{Zn}-\text{N}_{\text{pyridine}}$ , which may attribute to different coordination modes of sulfate anion.

From the above structure description, it is found that 1–5 contain 2,6-di(pyrazolyl)pyridine derivative ligands, the  $\text{SO}_4^{2-}$  anion and different metal ions. The differences of coordination

modes of the  $\text{SO}_4^{2-}$  anion and 2,6-di(pyrazolyl)pyridine derivative ligands lead to the distinction of the resultant structures. The  $(\text{HL}^1)^-$  ligand in complexes 1–3 has only one kind of the coordination mode, which act as a quadridentate ligand (Supporting Information Figure S12a). However, the  $\text{H}_2\text{L}^2$  ligand in complexes 4 and 5 has two kinds of the coordination modes, which acts as quadridentate and tridentate fashions, respectively (Supporting Information Figures S12b and S12c). On the other hand, coordination sulfate anion in complexes 1–4 has also different coordination modes. The most common  $\mu_2$ -bridging mode is found in complexes 1, 2, and 4 (Scheme 2f), while the sulfate anion in complex 3 acts as a  $\mu_4$ -bridging mode (Scheme 2c), which is very rare. In addition, sulfate anion in complex 5 does not directly coordinate to the metal. The different coordination modes of sulfate anion result in different structural characterization of the complexes. To the best of our knowledge, during constructing inorganic–organic open-framework compounds, sulfate group plays an important role, which can form one, two, and three-dimensional stable coordination polymer structures with relatively low valent metal ions.<sup>20,14b</sup> However, in the reaction system, if an *N*-heterocyclic chelate ligand was introduced, the sulfate anion could not form coordination polymer structures, while it could form discrete coordination structures with various coordination modes of sulfate anion.

**UV–vis Absorption Spectra.** The electronic absorption spectra of complexes 1–5 are recorded. As shown in Supporting Information Figure S10, electronic absorption spectra of the complexes 1, 3, 4, and 5 have similar absorption patterns. Bands at 260 nm for 1, 266 nm for 3, 262 nm for 4, and 258 nm for 5 belong to  $\pi$ – $\pi^*$  transition of ligand. Bands at 358 nm for 1, 380 nm for 3, 366 nm for 4, and 336 nm for 5 are ascribed to the LLCT (intraligand charge transfer) transitions.<sup>38</sup> The characterization absorption bands of complexes 1, 3, and 4 relative to that of the ligands move to slightly red-shift, and the order of corresponding energies is 3 (380 nm) < 4 (366 nm) < 1 (358 nm), which is probably attributed to different coordination modes of the ligands ( $\text{H}_2\text{L}^1$ ,  $\text{H}_2\text{L}^2$ , and  $\text{SO}_4^{2-}$ ). For complex 2, the high-frequency absorption band at 258 nm is assigned to  $\pi$ – $\pi^*$  transitions of  $\text{H}_2\text{L}^1$  ligand. The band at 482 nm is attributed to the LLCT with LMCT (ligand to metal charge transfer) transition. Bands at 612, 792, 834 nm are assigned to the  $d$ – $d^*$  transition of Co atom, shown in Supporting Information Figure S11.

**Quantum Chemistry Calculations of Complexes 1, 3, and 4.** According to molecular orbital theory, the frontier orbitals and nearby molecular orbitals are the most important factors for the stability. The larger difference between the frontier orbitals, the more stable the molecular structure.<sup>39–41</sup> The frontier molecular orbital symmetry and eigenvalues in Hartree for the complexes 1, 3, and 4 (See Supporting Information Table S1): the highest occupied molecular orbital (HOMO) –3.55, –1.68, and –3.19 eV; the lowest unoccupied molecular orbital (LUMO) –1.92, –1.54, and –1.90 eV. The energy gap value ( $\Delta E = E_{\text{LUMO}} - E_{\text{HOMO}}$ ) for the complexes 1, 3, and 4 is 1.63, 0.14, and 1.29 eV, respectively. It is shown that the order of thermodynamic stability about the complexes is 1 > 4 > 3. This is an agreement with the UV–vis spectra analysis result. The atomic net charges and electron configuration for the complexes 1, 3, and 4 calculated in the NBO analysis are listed in Supporting Information Tables S2–S6. The net charges of zinc atoms in the complexes 1, 3, and 4 are in the range from 1.024 to 1.061e, deviating from its oxidation valence (+2). This

is showing that the metal zinc obtained partly electron from the ligand ( $\text{H}_2\text{L}^1$  or  $\text{H}_2\text{L}^2$ ) and the sulfate anion. The average net charges of the coordinated oxygen atoms from the sulfate anion (–0.705e for complex 1, –0.690e for complex 4) are more negative than that of the uncoordinated oxygen atoms from the same sulfate anion (–0.610e for complex 1, –0.604e for complex 4). In complexes 1, 3, and 4, the average net charges of the coordinated nitrogen atoms from pyridine ring are –0.654, –0.700, and –0.655e, respectively; the average net charges of the terminal coordinated and uncoordinated nitrogen atoms from pyrazolyl rings are –0.341, –0.414, –0.367e and –0.379, –0.387, –0.406e, respectively; while the average net charges of the coordinated nitrogen atoms acting as a bridging from pyrazolyl rings for complexes 1, 3, and 4 are –0.435, –0.450, –0.438e, respectively, showing that the order of the average net charge of nitrogen atoms in complexes 1 and 4:  $N_{\text{pyridine}} < N_{\text{bridge(pyrazolyl)}} < N_{\text{uncoordinated(pyrazolyl)}} < N_{\text{terminalcoordinated(pyrazolyl)}}$ . However, in complex 3,  $N_{\text{pyridine}} < N_{\text{bridge(pyrazolyl)}} < N_{\text{terminalcoordinated(pyrazolyl)}} < N_{\text{uncoordinated(pyrazolyl)}}$ , which may attribute to different coordination modes of the sulfate anion.

**Thermal Properties.** To examine the thermal stability of complexes 1 and 3–5, thermal gravimetric analyses (TGA) was carried out at a heating rate of 10 °C/min under atmosphere in the temperature range of 45–1000 °C (Supporting Information Figure S13). In complex 1, the result shows the initial weight loss of 4.46% before 205 °C is due to the release of one lattice water molecule and one free ethanol molecule (calcd 3.25%). So the framework is stable up to 205 °C. The second weight loss occurs in the temperature range of 205–641 °C, which is ascribed to the release of four  $(\text{HL}^1)^-$  ligands and two  $\text{SO}_4^{2-}$  anions. Finally the remaining weight corresponds to the formation of ZnO (obsd 16.25%, calcd 16.55%). The thermal stability behavior of complexes 3–5 is similar to that of the complex 1.

**Photoluminescent Properties.** The solid-state photoluminescent spectra of the complexes 1–5 and their corresponding ligands at room temperature were examined, respectively, as shown in Figures 6 and 7. Complex 1 displays a broad emission band at 437 nm upon excitation at 368 nm with a slit width (1:1), a red shift of about 80 nm relative to that of the  $\text{H}_2\text{L}^1$  ligand (a strong emission band at 357 nm upon excitation 337 nm with a slit width (1:1)). Similar to 1, complex 3 also exhibits a broad emission peak at 452 nm upon excitation at 398 nm with a slit width (3:1), a red shift of 95 nm relative to that of

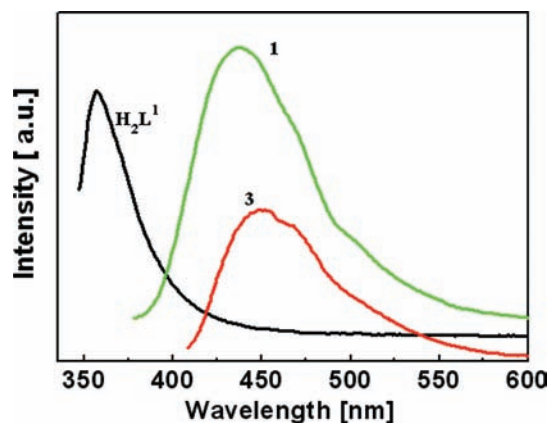


**Figure 6.** Solid-state photoluminescence spectra of  $\text{H}_2\text{L}^1$ , 1, and 3 at room temperature.

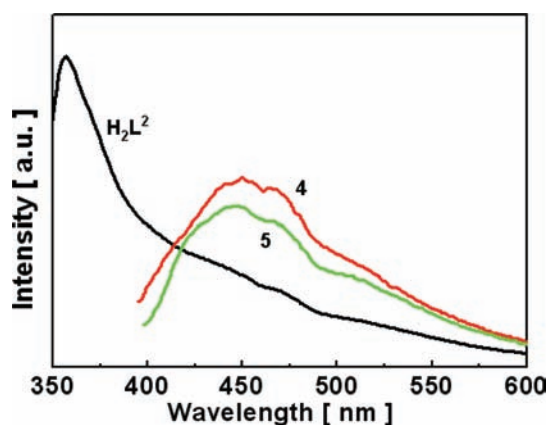


Figure 7. Solid-state photoluminescence spectra of  $H_2L^2$ , 4, and 5 at room temperature.

the  $H_2L^1$  ligand. When excited at 385 nm, 4 and 5 display bluish violet emissions with emission maxima at 441 and 446 nm, respectively, with the same slit width (3:1). It is clear that the emissions of complexes 4 and 5 are faintish than that of  $H_2L^2$ . While, the complexes 4 and 5 exhibit similar shapes of the emission spectra. It is shown that the emissions of the complexes 4 and 5 are mainly origin from ligand  $H_2L^2$  moiety. In contrast to the emission wavelength of the free ligand  $H_2L^2$  ( $H_2L^2$  is excited at 335 nm with emissions at 357 nm), there are red-shifted of 94 and 99 nm for the two complexes, respectively. In view of the luminescence of free neutral ligands and previously reported Zn(II) coordination polymers, the emission of the complexes 1, 3, 4, and 5 occurs red-shifted, which is probably due to the ligand to metal charge transfer (LMCT).<sup>42–45</sup>

**Catalysis Study.** In the primary stage of our work, the oxidation reaction of cyclohexane was employed as a model reaction and complex 1 was examined as a catalyst. The reaction was carried out in solvent of  $CH_3CN$  at 40 °C. It showed small TON value, indicating selectivity of the catalysts for the reaction of cyclohexane conversion is lower. While, by a blank experiment being conducted in the absence of the catalyst, under the above reaction conditions, the result found that no products were detected. For the sake of comparison, complexes 2–5 were also used as catalysts. As shown in Table 5, similarly, there is very low catalytic activity with TON value in the range of 1.07–9.31, although cyclohexane can reach high conversion after the reaction for some time. It is found that the order of the catalyst activity is  $4 > 5 > 3 > 2 > 1$  by comparing the catalysts activity of complexes 1–5. In particular, the catalytic efficiency of the complexes 4 and 5 is found to be

much better than that of 1 and 2, and the observed enhancement in catalytic activity is attributable to different substituted groups of 2,6-di(3-pyrazolyl)pyridine derivative ligands. This is because that substituted methyl group on pyrazolyl moiety is favorable to the catalytic reaction to produce cyclohexanol and cyclohexanone.

## CONCLUSIONS

In this work, five new complexes supported by 2,6-bis(3-pyrazolyl)pyridine-derived ligands have been successfully synthesized for the first time under the hydrothermal conditions by fine changing solvent and controlling pH value. In the reaction process, it is found that the amounts of aliphatic dicarboxylic acid may influence the coordination configuration of sulfate anion. X-ray analysis reveals that molecules in the complexes 1 and 4 form a 1D chain via intra- or intermolecular hydrogen bonds; however, two adjacent molecules in the complexes 2 and 3 can only generate a supermolecular dimer through intra- or intermolecular hydrogen bonds. Spectra analysis shown that complexes 1, 3, 4, and 5 possessed stronger fluorescence properties and they could be anticipated as potential fluorescent materials; in addition, we also investigated primary catalytic activity of complexes 1–5 by the oxidation reactions of cyclohexane.

## ASSOCIATED CONTENT

### Supporting Information

PXRD patterns and TG curves of the complexes 1 and 3–5 are shown in Figures S1–S4 and S13. Figures S5–S9, S10–S11, and S12 present the infrared spectra, UV–vis spectra, and the coordination modes of  $H_2L^1$  and  $H_2L^2$  ligands of complexes 1–5, respectively. The frontier molecular orbital symmetry and eigenvalues in Hartree for complexes 1, 3, and 4 are listed in Table S1. The atomic net charges and electron configurations for the complexes 1, 3, and 4 calculated in the NBO analysis are presented in Tables S2–S4. This material is available free of charge via the Internet at <http://pubs.acs.org>. Tables of atomic coordinates, isotropic thermal parameters, and complete bond distances and angles have been deposited with the Cambridge Crystallographic Data Center. Copies of this information may be obtained free of charge, by quoting the publication citation and deposition numbers CCDC 807813 (1), 807814 (2), 807815 (3), 807816 (4), and 807817 (5) from the Director, CCDC, 12 Union Road, Cambridge, CB2 1EZ, UK (fax +44-1223-336033; e-mail [deposit@ccdc.cam.ac.uk](mailto:deposit@ccdc.cam.ac.uk); <http://www.ccdc.cam.ac.uk>).

Table 5. Data of Oxidation for Cyclohexane with Complexes 1–5/ $H_2O_2$ / $HNO_3$ / $CH_3CN$  at 40 °C<sup>a</sup>

catalysts	mole ratio			time (h)	reaction medium	cyclohexane conversion (%)	TON <sup>b</sup> (cyclohexanol and cyclohexanone)
	catalyst/cyclohexane ( $10^{-5}$ )	catalyst/ $H_2O_2$ ( $10^{-6}$ )	catalyst/ $HNO_3$ ( $10^{-4}$ )				
1	6.52	2.5	5	4	$CH_3CN$	99.15	5.28
2	6.52	2.5	5	4	$CH_3CN$	98.89	2.26
3	6.52	2.5	5	4	$CH_3CN$	99.56	1.07
4	6.52	2.5	5	4	$CH_3CN$	96.91	9.31
5	6.52	2.5	5	4	$CH_3CN$	97.30	8.53

<sup>a</sup>1:  $[Zn_2(HL^1)_2(\mu_2-SO_4)]_2 \cdot EtOH \cdot H_2O$ . 2:  $[Co_2(HL^1)_2(\mu_2-SO_4)]_2 \cdot 2DMF \cdot 6H_2O$ . 3:  $[Zn_4(HL^1)_4(\mu_4-SO_4)] [OH]_2$ . 4:  $[Zn_2(HL^2)_2(\mu_2-SO_4)] \cdot 2H_2O$ . 5:  $[Zn(H_2L^2)(H_2O)_2] \cdot (SO_4) \cdot 0.87H_2O$ . <sup>b</sup>TON: moles of products (cyclohexanol and cyclohexanone)/moles of catalysts.

## ■ AUTHOR INFORMATION

## Corresponding Author

\*E-mail: yhxing2000@yahoo.com.

## Notes

The authors declare no competing financial interest.

## ■ ACKNOWLEDGMENTS

This work was supported by grants of the National Natural Science Foundation of China (No. 21071071), the Dr. start Foundation of Liaoning province in China (No. 20111067), and the State Key Laboratory of Inorganic Synthesis and Preparative Chemistry, College of Chemistry, Jilin University, Changchun 130012, P.R. China (Grant No. 2010-15).

## ■ REFERENCES

- (1) (a) Xu, Y.; Chen, P. K.; Che, Y. X.; Zheng, J. M. *Eur. J. Inorg. Chem.* **2010**, *34*, 5478–5483. (b) Gong, Y.; Li, J.; Qin, J. B.; Wu, T.; Cao, R.; Li, J. H. *Cryst. Growth Des.* **2011**, *11*, 1662–1674. (c) Farha, O. K.; Malliakas, C. D.; Kanatzidis, M. G.; Hupp, J. T. *J. Am. Chem. Soc.* **2010**, *132*, 950–952. (d) Almeida Paz F. A.; Klinowski, J.; Vilela, S. M. F.; Tomé, J. P. C.; Cavaleiro, J. A. S.; Rocha, J. *Chem. Soc. Rev.* DOI: 10.1039/c1cs15055c. (e) Deng, H.; Doonan, C. J.; Furukawa, H.; Ferreira, R. B.; Towne, J.; Knobler, C. B.; Wang, B.; Yaghi, O. M. *Science* **2010**, *327*, 846–850. (f) Doonan, C. J.; Tranchemontagne, D. J.; Glover, T. G.; Hunt, J. R.; Yaghi, O. M. *Nature Chem.* **2010**, *2*, 235–238.
- (2) (a) Lv, Y.; Qi, Y.; Sun, L.; Luo, F.; Che, Y.; Zheng, J. *Eur. J. Inorg. Chem.* **2010**, *35*, 5592–5596. (b) Yu, W. S.; Cheng, C. C.; Cheng, Y. M.; Wu, P. C.; Song, Y. H.; Chi, Y.; Chou, P. T. *J. Am. Chem. Soc.* **2003**, *125*, 10799–10800. (c) Li, J. R.; Kuppler, R. J.; Zhou, H. C. *Chem. Soc. Rev.* **2009**, *38*, 1477–1504. (d) Ma, S. Q.; Zhou, H. C. *Chem. Commun.* **2010**, *46*, 44–53. (e) Zhao, D.; Yuan, D. Q.; Zhou, H.-C. *Energy Environ. Sci.* **2008**, *1*, 222–235. (f) Farha, O. K.; Hupp, J. T. *Acc. Chem. Res.* **2010**, *43*, 1166–1175.
- (3) (a) He, H.; Dai, F.; Sun, D. J. C. C. *Dalton Trans.* **2009**, *5*, 763–766. (b) Noveron, J. C.; Lah, M. S.; DelSesto, R. E.; Arif, A. M.; Miller, J. S.; Stang, P. J. *J. Am. Chem. Soc.* **2002**, *124*, 6613–6625.
- (4) (a) Zhao, Y. H.; Su, Z. M.; Fu, Y. M.; Shao, K. Z.; Li, P.; Wang, Y.; Hao, X. R.; Zhu, D. X.; Liu, S. D. *Polyhedron.* **2008**, *27*, 583–594. (b) Campbell, K.; Kuehl, C. J.; Ferguson, M. J.; Stang, P. J.; Tykewinski, R. R. *J. Am. Chem. Soc.* **2002**, *124*, 7266–7267.
- (5) (a) Rao, K. P.; Thirumurugan, A.; Rao, C. N. R. *Chem.—Eur. J.* **2007**, *13*, 3193–3201. (b) Banu, K. S.; Mondal, S.; Guha, A.; Das, S.; Chattopadhyay, T.; Suresh, E.; Zangrando, E.; Das, D. *Polyhedron.* **2011**, *30*, 163–168.
- (6) Halcrow, M. A. *Coord. Chem. Rev.* **2005**, *249*, 2880–2908.
- (7) (a) Zhou, Y.; Chen, W. J. C. C. *Dalton Trans.* **2007**, *44*, 5123–5125. (b) Roberts, T. D.; Tuna, F.; Malkin, T. L.; Kilner, C. A.; Halcrow, M. A. *Chem. Sci.* **2012**, *3*, 349–354. (c) Coronado, E.; Mascaros, J. R. G.; Almeida, M. C. G. M.; Waerenborgh, J. C. *Polyhedron* **2007**, *26*, 1838–1844. (d) Coronado, E.; Gimenez-Lopez, M. C.; Gimenez-Saiz, C.; Romero, F. M. *CrystEngComm* **2009**, *11*, 2198–2203.
- (8) (a) Zhou, Y.; Chen, W.; Wang, D. J. C. C. *Dalton Trans.* **2008**, *11*, 1444–1453. (b) Plaul, D.; Spielberg, E. T.; Plass, W. Z. *Anorg. Allg. Chem.* **2010**, *636*, 1268–1274. (c) Ghoochany, L. T.; Farsadpour, S.; Sun, Y.; Thiel, W. R. *Eur. J. Inorg. Chem.* **2011**, 3431–3437. (d) Wang, P.; Leung, C. H.; Ma, D. L.; Yan, S. C.; Che, C. M. *Chem.—Eur. J.* **2010**, *16*, 6900–6911.
- (9) (a) Zhao, B.; Shu, H.; Hu, H.; Qin, T.; Chen, X. J. *Coord. Chem.* **2009**, *62*, 1025–103. (b) Hu, S.; Zhao, Y.; Hu, H. M.; Liu, L. *Acta Crystallogr.* **2011**, *E67*, m945–m946. (c) Zheng, A. X.; Wang, H. F.; Lu, C. N.; Ren, Z. G.; Li, H. X.; Lang, J. P. J. C. C. *Dalton Trans.* **2012**, *41*, 558–566. (d) Wang, L.; Yang, Q.; Chen, H.; Li, R. X. *Inorg. Chem. Commun.* **2011**, *14*, 1884–1888.
- (10) Baker, A. T.; Craig, D. C.; Dong, G. *Inorg. Chem.* **1996**, *35*, 1091–1092.
- (11) Liu, P.; Zhou, Y. B.; Li, M. G.; An, C. X. *Acta Crystallogr.* **2008**, *E64*, o226.
- (12) Xiao, L. X.; Luo, Y. M.; Chen, Z.; Li, J.; Tang, R. R. *Spectrochimica Acta Part A* **2008**, *71*, 321–325.
- (13) (a) Constable, E. C. *Chem. Commun.* **1997**, 1073–1080. (b) Goshe, A. J.; Crowley, J. D.; Bosnich, B. *Helv. Chim. Acta* **2001**, *84*, 2971–2985. (c) Schubert, U. S.; Eschbaumer, C. *Angew. Chem., Int. Ed.* **2002**, *41*, 2892–2926.
- (14) (a) Ng, C. H.; Lim, C. W.; Teoh, S. G.; Fun, H. K.; Usman, A.; Ng, S. W. *Inorg. Chem.* **2002**, *41*, 2–3. (b) Rao, C. N. R.; Behera, J. N.; Dan, M. *Chem. Soc. Rev.* **2006**, *35*, 375–387.
- (15) Yuan, D.; Xu, Y.; Hong, M.; Bi, W.; Zhou, Y.; Li, X. *Eur. J. Inorg. Chem.* **2005**, 1182–1187.
- (16) Carlucci, L.; Ciani, G.; Proserpio, D. M.; Rizzato, S. *CrystEngComm* **2003**, *5*, 190–199.
- (17) (a) Huang, Z.; Song, H. B.; Du, M.; Chen, S. T.; Bu, X. H. *Inorg. Chem.* **2004**, *43*, 931–944. (b) Ferrer, S.; Lloret, F.; Bertomeu, I.; Alzueta, G.; Borrás, J.; García-Granda, S.; Liu-González, M.; Haasnoot, J. G. *Inorg. Chem.* **2002**, *41*, 5816–5821.
- (18) Bettencourt-Dias, A.; Scott, V. J.; Hugdal, S. *Inorg. Chim. Acta* **2010**, *363*, 4088–4095.
- (19) Vidovic, D.; Radulovic, A.; Jevtovic, V. *Polyhedron* **2011**, *30*, 16–21.
- (20) Pifferi, C.; Picchi, M. P.; Cini, R. *Polyhedron* **2000**, *19*, 69–76.
- (21) Mishra, I. G. S.; Silva, T. F. S.; Martins, L. M. D. R. S.; Pombeiro, A. J. L. *Pure Appl. Chem.* **2009**, *81*, 1217–1227.
- (22) (a) Kirillova, M. V.; Kirillov, A. M.; Reis, P. M.; Silva, J. A. L.; Fraústo da Silva, J. J. R.; Pombeiro, A. J. L. *J. Catal.* **2007**, *248*, 130–136. (b) Reis, P. M.; Silva, J. A. L.; Fraústo da Silva, J. J. R.; Pombeiro, A. J. L. *Chem. Commun.* **2000**, *19*, 1845–1846. (c) Reis, P. M.; Silva, J. A.; Palavra, A. A. F.; Fraústo da Silva, J. J. R.; Kitamura, T.; Fujiwara, Y.; Pombeiro, A. J. L. *Angew. Chem., Int. Ed.* **2003**, *42*, 821–823.
- (23) (a) Mishra, G. S.; Kumar, A. *Catal. Lett.* **2002**, *81*, 113–117. (b) Kumar, A.; Mishra, G. S.; Kumar, A. *Transition Met. Chem.* **2003**, *28*, 913–917.
- (24) Mishra, G. S.; Alegria, E. C. B.; Martins, L. M. D. R. S.; Fraústo da Silva, J. J. R.; Pombeiro, A. J. L. *J. Mol. Catal. A: Chem.* **2008**, *285*, 92–100.
- (25) Silva, T. F. S.; Luzyanin, K. V.; Kirillova, M. V.; Ftima Guedes da Silva, M.; Martins, L. M. D. R. S.; Pombeiro, A. J. L. *Adv. Synth. Catal.* **2010**, *352*, 171–187.
- (26) Datta, S.; Seth, D. K.; Butcher, R. J.; Bhattacharya, S. *Inorg. Chim. Acta* **2011**, *377*, 120–128.
- (27) Luo, Y.; Chen, Z.; Tang, R.; Xiao, L. *Chem. Reaction Eng. Technol.* **2006**, *22*, 549–553.
- (28) Luo, Y.; Xiao, L.; Chen, Z.; Huang, W.; Tang, X. *Chem. Res. Appl.* **2008**, *20*, 299–303.
- (29) Sheldrick, G. M. *SADABS, Program for Empirical Absorption Correction for Area Detector Data*; University of Göttingen: Göttingen, Germany, 1996.
- (30) Sheldrick, G. M. *SHELXS 97, Program for Crystal Structure Refinement*; University of Göttingen: Göttingen, Germany, 1997.
- (31) Becke, A. D. J. *Chem. Phys.* **1993**, *98*, 1372–1377.
- (32) Lee, C. T.; Yang, W. T.; Parr, R. G. *Phys. Rev. B* **1988**, *37*, 785–789.
- (33) Frisch, M. J.; Trucks, G. W.; Schlegel, H. B.; Scuseria, G. E.; Robb, M. A.; Cheeseman, J. R.; Montgomery, J. A., Jr.; Vreven, T.; Kudin, K. N.; Burant, J. C.; Millam, J. M.; Iyengar, S. S.; Tomasi, J.; Barone, V.; Mennucci, B.; Cossi, M.; Scalmani, G.; Rega, N.; Petersson, G. A.; Nakatsuji, H.; Hada, M.; Ehara, M.; Toyota, K.; Fukuda, R.; Hasegawa, J.; Ishida, M.; Nakajima, T.; Honda, Y.; Kitao, O.; Nakai, H.; Klene, M.; Li, X.; Knox, J. E.; Hratchian, H. P.; Cross, J. B.; Bakken, V.; Adamo, C.; Jaramillo, J.; Gomperts, R.; Stratmann, R. E.; Yazyev, O.; Austin, A. J.; Cammi, R.; Pomelli, C.; Ochterski, J. W.; Ayala, P. Y.; Morokuma, K.; Voth, G. A.; Salvador, P.; Dannenberg, J. J.; Zakrzewski, V. G.; Dapprich, S.; Daniels, A. D.; Strain, M. C.; Farkas, O.; Malick, D. K.; Rabuck, A. D.; Raghavachari, K.; Foresman, J. B.; Ortiz, J. V.; Cui, Q.; Baboul, A. G.; Clifford, S.; Cioslowski, J.; Stefanov, B. B.; Liu, G.; Liashenko, A.; Piskorz, P.; Komaromi, I.

Martin, R. L.; Fox, D. J.; Keith, T.; Al-Laham, M. A.; Peng, C. Y.; Nanayakkara, A.; Challacombe, M.; Gill, P. M. W.; Johnson, B.; Chen, W.; Wong, M. W.; Gonzalez, C. Pople, J. A. *Gaussian 03*, Revision B.05; Gaussian, Inc., Wallingford CT, 2004.

(34) Hay, P. J.; Wadt, W. R. *J. Chem. Phys.* **1985**, *82*, 299–310.

(35) Addison, A. W.; Rao, T. N. *J. Chem. Soc., Dalton Trans.* **1984**, 1349–1356.

(36) Huang, X.; Yang, Z.; Yang, X. J.; Zhao, Q.; Xia, Y.; Wu, B. *Inorg. Chem. Commun.* **2010**, *13*, 1103–1107.

(37) Carlucci, L.; Ciani, G.; Proserpio, D. M.; Rizzato, S. *CrystEngComm* **2003**, *5* (34), 190–199.

(38) Li, Z. P.; Xing, Y. H.; Cao, Y. Z.; Zeng, X. Q.; Ge, M. F.; Niu, S. Y. *Polyhedron* **2009**, *28*, 865–874.

(39) Chattaraj, P. K.; Roy, D. R.; Elango, M.; Subramanian, V. *J. Phys. Chem. A* **2005**, *109* (42), 9590–9597.

(40) Aihara, J. *J. Phys. Chem. A* **1999**, *103*, 7487–7495.

(41) Yoshida, M.; Aihara, J. *Phys. Chem. Chem. Phys.* **1999**, *1*, 227–230.

(42) Li, S. L.; Lan, Y. Q.; Ma, J. F.; Fu, Y. M.; Yang, J.; Ping, G. J.; Liu, J.; Su, Z. M. *Cryst. Growth Des.* **2008**, *8*, 1610–1616.

(43) Su, Z.; Xu, J.; Fan, J.; Liu, D. J.; Chu, Q.; Chen, M. S.; Chen, S. S.; Liu, G. X.; Wang, X. F.; Sun, W. Y. *Cryst. Growth Des.* **2009**, *9*, 2801–2811.

(44) Wang, X. L.; Qin, C.; Wang, E. B.; Li, Y. G.; Hao, N.; Hu, C. W.; Xu, L. *Inorg. Chem.* **2004**, *43*, 1850–1856.

(45) Cao, X. Y.; Zhang, J.; Li, Z. J.; Chen, J. K.; Yao, Y. G. *CrystEngComm.* **2007**, *9*, 806–817.